Stability analysis of nonholonomic multiagent coordinate-free formation control subject to communication delays

Antonio González*, Rosario Aragüés, Gonzalo López-Nicolás, Carlos Sagüés *

Instituto de Investigación en Ingeniería de Aragón, Universidad de Zaragoza, María de Luna 1, 50018 Zaragoza, Spain

SUMMARY

This paper investigates the convergence of nonholonomic multiagent coordinate-free formation control to a prescribed target formation subject to communication delays by means of Lyapunov-Krasovskii approaches and smooth state-feedback control laws. As a result, an iterative algorithm based on Linear Matrix Inequalities (LMI) is provided to obtain the worst-case point-to-point delay under which the multiagent system is guaranteed to be stable. It is worth mentioning that: (i) the given algorithm holds for any connected communication topology, (ii) the formation control is coordinate-free, that is, a common frame is not required to be shared between agents. The effectiveness of the given method is illustrated through simulation results. Copyright © 2010 John Wiley & Sons, Ltd.

1. INTRODUCTION

1.1. Background and motivation

In the context of multi-agent systems, the formation control problem [1] can be roughly defined as the achievement and maintenance of some prescribed geometrical formation shape in the space. An extensive number of fields and engineering applications in which the formation control appears can be mentioned in this respect: autonomous multivehicle control [2], cooperative control [3], unmanned aerial vehicles formation [4],[5], etc.

Formation control can be basically implemented under two approaches: (i) in terms of absolute positions [6, 7], and (ii) in terms of relative interagent distances [8] or relative interagent position vectors [9, 10, 11]. The latter case offers the advantage that there is no need to make the agents compute and share any global common frame. This coordinate-free implementation increases the flexibility and autonomy. For instance, the agents can operate in a GPS-denied environment by using the locally referred information coming from their independent onboard sensors.

On the other hand, a multiagent team constitutes a networked system, in which the agents interact among them via communications. Therefore, a relevant issue to take into consideration in the stability analysis of formation control systems is the presence of time delays [12, 13], which mainly appear due to multi-hop communication between agents. Typical examples can be found in different related applications: formation of unmanned aerial vehicles [4], synchronization of flying spacecraft [14], formation of mobile robots through network systems [15], etc.

It is known that the complexity of the dynamics of a multiagent system subject to communication delays does not lend itself for simple mathematical stability analysis. With the aim to reduce the complexity of the problem, linear models are usually taken into account to describe the dynamics of each individual agent: single integrator [16], double-integrator [17] or even high-order models [18]. Nevertheless, linear models cannot be used to describe the kinematics of unicycle or car-like

robots, for instance, because of the existence of nonholonomic constraints. Some recent results involving nonholonomic systems subject to communication delays have been addressed: [19] and [20] investigate the output feedback control design of nonholonomic systems with chained structure and high order dynamics, respectively. Other related contributions with formation control can be found in [21], where a non-coordinate-free formation control strategy of nonholonomic system with communication delays under feedback linearization is proposed. However, an exhaustive research on numerical efficient and reliable methods to compute a worst-case for time delays is not carried out in these latter works. Altough an analytical expression for the worst-case point-to-point delay was provided in [16] for the coordinate-free formation control under communication delays, the study is restricted to single-integrator models for the kinematic's agent and a complete communication topology. The formation control was further extended to partial communication graphs and systems with nonholonomic constraints [22], but the problem of communication delays is not considered there. Motivated by the negative effects of time delays on the stability and performance of such control systems, we focus on the stability analysis of coordinate-free formation nonholonomic control systems under communication delays and smooth state-feedback control strategies. It should be noticed that, in the case of single integrators, the stability analysis problem is easier to deal with because the resulting system model is linear, and therefore it can be addressed via standard quadratic Lyapunov approaches. However, the nonlinear dynamics of unicycles, altogether with the distributed and interconnected structure of the multiagent system and the presence of time delays, make the stability analysis a complex issue, which to the best author's knowledge, has not been fully investigated.

1.2. Contributions

For a suitably designed smooth state-feedback control law subject to communication delays, we develop a sufficient condition based on Lyapunov-Krasovskii approaches [23] and Linear Matrix Inequalities (LMI) [24] to ensure the global asymptotic convergence of the nonholonomic multiagent system to the prescribed target formation subject to communication delays. Based on the obtained condition, we develop an iterative algorithm to easily obtain the worst-case point-to-point delay of the multiagent system under which the global stability is ensured. It is worth pointing out that LMI's can be easily solved by numerical efficient and reliable algorithms based on convex optimization approaches (e.g, interior-point [25]), available in standard commercial libraries: LMI Control Toolbox [26], SEDUMI [27], etc. It is also noteworthy the following aspects:

- Differently to other similar results in formation control with communication delays [16], where the communication topology is complete, we assume a partial communication topology with the only requirement to be connected. Therefore, not necessarily all the information concerning the relative interagent position measurements must be availabe by each agent.
- All the delayed vector position measurements are relative and referred to each agent's local frame. This feature allows to reduce the dependence on complex and expensive sensing and increases the agent's autonomy since the absolute position or orientation information is not required. Furthemore, it also brings more flexibility, by permitting operation in GPS-denied environments.
- It is well known that nonholonomic systems cannot be stabilized by stationary continuous state-feedback, as pointed out in [28], despite being controllable. As a consequence, the well-developed smooth nonlinear control theory and methodology cannot be directly used to such systems. In this work, a smooth control law is given by overcoming the obstruction of stabilizability contained in Brockett's theorem [29] using a coordinate transformation to polar coordinates [30, 31, 32].

1.3. Organization

The remainder of the paper is organized as follows: we start with the problem statement in Section 2.1. Some preliminary notation and results are given in Section 2.2. In Section 3, we describe the proposed control law under analysis. In Section 4, we present the main results, consisting of the

stability analysis in terms of the worst-case point-to-point delay by means of Lyapunov-Krasovskii approaches. Section 5 is devoted to illustrate the effectiveness of the proposed method through simulation results. Finally, some concluding remarks and perspectives are gathered in Section 6.

2. PROBLEM STATEMENT AND PRELIMINARIES

2.1. Problem statement

Consider a nonholonomic multiagent system formed by N unicycles. The kinematics model of each agent $1 \leq i \leq N$, expressed in some arbitrary reference frame, is given below:

$$\begin{bmatrix} \dot{q}_{i,x} \\ \dot{q}_{i,y} \\ \dot{\phi}_i \end{bmatrix} = \begin{bmatrix} cos(\phi_i) & 0 \\ sin(\phi_i) & 0 \\ 0 & 1 \end{bmatrix} \begin{bmatrix} v_i \\ w_i \end{bmatrix}, \tag{1}$$

where the vector $q_i = (q_{i,x}, q_{i,y})$ contains the x-y coordinates of the ith agent's position vector, and ϕ_i represents the angular orientation. The agent's motion is controlled respectively by the linear velocity v_i and the angular velocity w_i.

The formation control problem has the objective to design the control laws for v_i and w_i to force the multiagent system (1) to converge to a prescribed target formation, defined by the following set of interagent position vectors:

$$c_{ji} = (c_{ji,x}, c_{ji,y}), \ \forall [i,j] \in [1, ..., N] \times [1, ..., N], \ i \neq j, \tag{2}$$

where c_{ji} is the prescribed relative position vector between two pairs of agents i and j. The following two parameters play a key role in our analysis:

- (i) The norm of the relative interagent position error ρ_{ji}:

$$\rho_{ji} = ||q_{ji} - c_{ji}||, \tag{3}$$

  where $q_{ji} = q_j - q_i$ is the current relative position vector between agents j and i, and c_{ji} is the prescribed relative position vector (2).
- (ii) The relative misalignment angular error α_{kji}:

$$\alpha_{kji} = \phi_k - \psi_{ji}, \tag{4}$$

  where α_{kji} is here defined as the angular difference between the kth agent's orientation ϕ_k and the interagent angular error ψ_{ji} between agent j and i: $\psi_{ji} = atan2 \left(q_{ji,y} - c_{ji,y}, \ q_{ji,x} - c_{ji,x}\right)$. **The function** $atan2 : \mathcal{R}^2 \to (-\pi, \pi]$ **is equivalent to a four-quadrant arctangent function [33, 34], defined as:**

$$atan2(y, x) = \begin{cases} 0 & (x,y) = (0,0) \\ arctg(y/x) + (\pi/2)sign(y)(1 - sign(x)) & \textbf{otherwise,} \end{cases}$$

where $sign(a) = \begin{cases} 1 & \textbf{if } a \geq 0 \\ -1 & \textbf{if } a < 0. \end{cases}$

The geometrical description of ρ_{ji} and α_{kji} is depicted in Fig. 1.

Remark 1

Definition 1
The adjacency matrix which describes the communication graph on the multiagent system (1) is
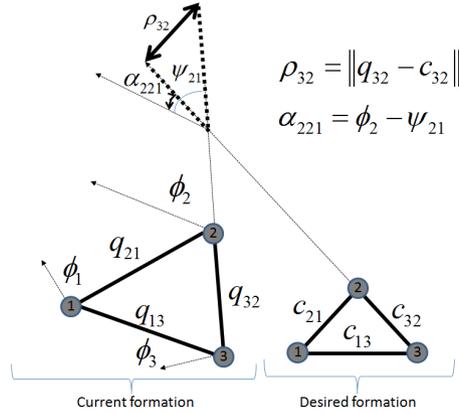
Figure 1. Geometrical description of the norm of relative interagent error position ρ_{ji} and the relative angular misalignment errors α_{kji}, referred to any arbitrary reference frame. In the picture, ρ_{32} and α_{221} have been specifically highlighted.

defined as:

$$\mathcal{A} = \begin{bmatrix} 0 & a_{12} & \cdots & a_{1N} \\ a_{21} & 0 & \cdots & a_{2N} \\ \cdots & \cdots & \cdots & \cdots \\ a_{N1} & a_{N2} & \cdots & 0 \end{bmatrix} \in \{0,1\}^{N \times N}, \tag{5}$$

where $a_{ij} = a_{ji} = 1$ if the communication link between agent i and j is active, and $a_{ij} = a_{ji} = 0$ otherwise.

Definition 2
Given two agents i and j with an active communication link $a_{ij} = a_{ji} = 1$, we denote $d_{ij} = d_{ji} > 0$ as the time delay induced by the communication link between both agents. The worst-case point-to-point delay τ is defined as $\tau = \max\limits_{i,j/a_{ij}=1} (d_{ij})$.

The objective on this paper is to develop a systematic method to obtain the worst-case point-to-point delay τ under which the multiagent system (1) is ensured to be globally stable. The proposed control strategy for our analysis is next given in Section 3.

2.2. Preliminary notation and materials

Let I_n be the $n \times n$ identity matrix, $0_{n \times m}$ be a $n \times m$ matrix with all its entries equal to 0, and $1_{n \times m}$ be a $n \times m$ matrix with all its entries equal to 1. Given a set of scalars or matrices of compatible dimensions $\gamma_{ij}, 1 \leq i \leq m, 1 \leq j \leq n$, we denote $[\gamma_{ij}]_{m,n}$ as the m-by-n block matrix $\begin{bmatrix} \gamma_{11} & \cdots & \gamma_{1n} \\ \cdots & \cdots & \cdots \\ \gamma_{m1} & \cdots & \gamma_{mn} \end{bmatrix}$. Given a vector $v = [v_1, ..., v_n]$, the shortcut $diag(v)$ denotes the $n \times n$ diagonal matrix, where the diagonal entries are respectively $v_1, .., v_n$. Given a set of N matrices: $J_1, ..., J_N$, the shortcut $diag(J_1, ..., J_N)$ denotes a block-diagonal matrix, where the diagonal entries are respectively $J_1, ..., J_N$.

The following lemma will be useful later, in the proof of the main results:

Lemma 1
Given two square matrices A and B, the following equivalence holds:

$$\mathcal{P}^T (A \otimes B) \mathcal{P} = B \otimes A \tag{6}$$

where $\mathcal{P}$ is some regular permutation matrix, and the symbol $\otimes$ stands for the Kronecker product.

3. CONTROL LAW DEFINITION

For our stability analysis, we propose the following control law for each agent $1 \leq i \leq N$ [†]:

$$v_i = K_1 \sum_j a_{ji} \rho_{ji}^{d_{ji}} cos(\alpha_{iji}^{d_{ji}}) \tag{7}$$

$$w_i = -\sum_j \tilde{a}_{ji} \left(K_2 sin(\alpha_{iji}^{d_{ji}}) + \frac{v_i^{d_{ji}} sin(\alpha_{iji}^{d_{ji}})}{\rho_{ji}^{d_{ji}}} + \frac{v_j^{d_{ji}} sin(\alpha_{jij}^{d_{ji}})}{\rho_{ji}^{d_{ji}}} \right),$$

where $\rho_{ji}^{d_{ji}}$ is the delayed norm of the relative interagent position error (3), $\alpha_{iji}^{d_{ji}}, \alpha_{jij}^{d_{ji}}$ are the delayed relative misalignment angular errors (4), and $v_i^{d_{ji}}, v_j^{d_{ji}}$ are the delayed linear velocities. Given two agents i, j, these parameters are assumed to be measurable (provided that $a_{ij} = a_{ji} = 1$) and subject to time delays d_{ji} given in Definition 2. In addition, K_1, K_2 are the control gains, a_{ji} are the coefficients of the adjacency matrix (5), and $\tilde{a}_{ji}$ are the coefficients of the following matrix:

$$\tilde{\mathcal{A}} = \begin{bmatrix} 0 & \tilde{a}_{12} & \cdots & \tilde{a}_{1N} \\ \tilde{a}_{21} & 0 & \cdots & \tilde{a}_{2N} \\ \cdots & \cdots & \cdots & \cdots \\ \tilde{a}_{N1} & \tilde{a}_{N2} & \cdots & 0 \end{bmatrix} \in \{0,1\}^{N \times N}, \tag{8}$$

whose values are defined as:

$$\tilde{a}_{ij} = \begin{cases} 1 & if \; j = \min_{1 \leq p \leq N} p \; / \; a_{ip} = 1 \\ 0 & otherwise. \end{cases} \tag{9}$$

Note from (9) the following properties:

$$(i): \sum_j \tilde{a}_{ij} = 1, \forall i = 1, ..., N, \qquad (ii): \tilde{a}_{ij} = 1 \Longrightarrow a_{ij} = 1, \; \forall i, j. \tag{10}$$

From the condition (i), it can be deduced that all the elements of each row of $\tilde{\mathcal{A}}$ are equal to 0 except for only one of them, which is equal to 1. It means that, from all the available measurements corresponding to the set of neighbor agents $j = 1, ..., N \; / \; a_{ij} = a_{ji} = 1$, only one of them is used to implement w_i, whose index j corresponds to the unique coefficient $\tilde{a}_{ij} = 1$ for each row i. The condition (ii) imposes that the communication link between agent i and j must be active, such that the agent i can receive the corresponding measurements from agent j.

The following assumptions are thereafter considered:

Assumption 1
The communication topology of the multiagent system is undirected and connected. It implies that all the agents keep at least one active link. In other words, the communication graph always contains a spanning tree.

Assumption 2
The angular velocities $\frac{d}{dt}\alpha_{kji}$ and w_i, $\forall i, j, k \in [1, ..., N] \times [1, ..., N] \times [1, ..., N]$ cannot exceed a limit given by σ: $\left| \frac{d}{dt}\alpha_{kji} \right| \leq \sigma$, $|w_i| \leq \sigma$, where σ is a positive scalar whose value is determined by power limitation on the actuators. Indeed, in real systems, no actuator could provide an infinity control force.

Remark 2
Note that the relative measurements $\rho_{ji}^{d_{ji}}, \alpha_{iji}^{d_{ji}}, \alpha_{jij}^{d_{ji}}$ in (7) are independent of the arbitrary reference frame used to express (1). This fact can be illustrated as follows:

[†]Numerical problems from possible division by zero in the control law implementation for w_i in (7) can be circumvented by applying an upper bounding such that $|w_i| \leq \sigma$ (see Assumption 2).

Consider two agents i and j, and their respective position vectors: q_i, q_j. Also, consider the kth agent's orientation ϕ_k, the interagent angular error ψ_{ji}, and the desired interagent position vector c_{ji}, all of them referred to some arbitrary coordinate reference frame. Now, given some arbitrary angle ϑ and vector q_t, consider a new coordinate reference frame subject to a rotation ϑ and translation q_t with respect to the original reference frame. It is easy to see that all the above magnitudes can be expressed in the rotated reference frame as:

$$q_i^* = R(\vartheta)q_i - q_t, \quad q_j^* = R(\vartheta)q_j - q_t, \quad c_{ji}^* = R(\vartheta)c_{ji} - q_t, \tag{11}$$
$$\phi_k^* = \phi_k + \vartheta, \quad \psi_{ji}^* = \psi_{ji} + \vartheta,$$

where $R(\vartheta)$ is the rotation matrix:

$$R(\vartheta) = \begin{bmatrix} cos(\vartheta) & -sin(\vartheta) \\ sin(\vartheta) & cos(\vartheta) \end{bmatrix}. \tag{12}$$

It is easy to see that:

$$\rho_{ji}^* = ||q_{ji}^* - c_{ji}^*|| = ||R(\vartheta)q_{ji} - q_t - R(\vartheta)c_{ji} + q_t|| = ||R(\vartheta)|| \, ||q_{ji} - c_{ji}|| = \rho_{ji}, \tag{13}$$
$$\alpha_{kji}^* = \phi_k^* - \psi_{ji}^* = \psi_k + \vartheta - \psi_{ji} - \vartheta = \alpha_{kji}.$$

From (13), it can be seen that the overall formation control system is coordinate-free, that is, no global reference frame is required to implement the proposed formation control strategy.

Remark 3
One positive aspect of delays is that the problem of dead-loop phenomenon in the control law (7) is circumvented [35, 36]. Given two agents i and j, the dead-loop comes from the fact that the agent i needs v_j to compute w_i, and the agent j needs v_i to compute w_j. Nevertheless, this is not a problem since the delayed linear velocities $v_i^{d_{ji}}$, $v_j^{d_{ji}}$ are used in (7).

The following results will be useful to obtain a state-space model of the overall multiagent system expressed in terms of the relative errors above defined ρ_{ji} and α_{kji}:

Lemma 2
The time-derivative of ρ_{ji} can be expressed as:

$$\dot{\rho}_{ji} = -cos(\alpha_{jij})v_j - cos(\alpha_{iji})v_i \tag{14}$$

Proof
See Appendix 7.1 $\qquad\qquad\qquad\qquad\qquad\qquad\qquad\qquad\qquad\qquad\qquad\qquad\qquad\qquad\qquad$ □

Lemma 3
The time-derivative of α_{kji} yields:

$$\dot{\alpha}_{kji} = \omega_k + \frac{1}{\rho_{ji}}sin(\alpha_{jij})v_j + \frac{1}{\rho_{ji}}sin(\alpha_{iji})v_i \tag{15}$$

Proof
See Appendix 7.2 $\qquad\qquad\qquad\qquad\qquad\qquad\qquad\qquad\qquad\qquad\qquad\qquad\qquad\qquad\qquad$ □

4. STABILITY ANALYSIS FOR MULTIPLE AGENTS WITH COMMUNICATION DELAYS:

The goal is to obtain the worst-case point-to-point delay τ (see Definition 2), such that the global asymptotic stability of the overall system (1) is guaranteed. The most unfavorable case is considered in our analysis by setting $d_{ij} = \tau$, $\forall i, j$. Before proceeding, we introduce the following results:

Theorem 1

For a given worst-case point-to-point delay τ, the system (1) is globally stable with the control law (7) if there exist scalars $\lambda, \mu, \varepsilon_1, \varepsilon_2 > 0$ such that the following LMI is fulfilled [‡]:

$$\begin{bmatrix} \Xi_1 & \Xi_2 & \Xi_3^T \Xi_4 \\ (*) & \Xi_4 & 0 \\ (*) & (*) & \Xi_4 \end{bmatrix} < 0 \tag{16}$$

where

$$\Xi_1 = \begin{bmatrix} -\lambda I_2 & \tilde{\Gamma}_1 + \lambda I_2 & 0_2 \\ (*) & -\lambda I_2 & 0_2 \\ (*) & (*) & -\lambda \tau^2 I_2 \end{bmatrix}, \Xi_2 = \begin{bmatrix} G_1 & 0_{2\times 1} & 0_2 \\ 0_{2\times 1} & 0_{2\times 1} & 0_2 \\ 0_{2\times 1} & G_2 & G_3 \end{bmatrix}, \tag{17}$$

$$\Xi_3 = \begin{bmatrix} 0_{1\times 2} & H_1 & 0_{1\times 2} \\ H_2 & 0_{1\times 2} & 0_{1\times 2} \\ 0_2 & H_3 & 0_2 \end{bmatrix}, \Xi_4 = \begin{bmatrix} -1 & 0 & 0_{1\times 2} \\ (*) & -\varepsilon_1 & 0_{1\times 2} \\ (*) & (*) & -\varepsilon_2 I_2 \end{bmatrix},$$

$$\tilde{\Gamma}_1 = \begin{bmatrix} -\frac{1}{4} K_1 & 0 \\ 0 & -\frac{1}{2} \mu K_2 \end{bmatrix},$$

$$G_1 = \frac{1}{4} \mu \delta_1 \sqrt{\tau} \begin{bmatrix} 0 \\ 1 \end{bmatrix}, \quad G_2 = \delta_2 \lambda \tau \begin{bmatrix} 1 \\ 0 \end{bmatrix}, \quad G_3 = -\frac{1}{2} K_1 \delta_3 \lambda \tau \cdot I_2,$$

$$H_1 = \sqrt{\tau} \begin{bmatrix} 1 & 0 \end{bmatrix}, \quad H_2 = \tau \begin{bmatrix} 1 & 0 \end{bmatrix}, \quad H_3 = \tau \begin{bmatrix} 1 & 0 \\ 0 & 2\frac{K_2}{K_1} \end{bmatrix},$$

$$\delta_1 = \sigma N, \quad \delta_2 = \sigma N, \quad \delta_3 = 2N.$$

Proof

See Appendix 7.3. □

Corollary 1

For a sufficiently small delay $\tau > 0$ and any positive control gains K_1 and K_2, the LMI (16) always holds.

Proof

Taking into account that $\Xi_4 < 0$ (see (17)), we apply Schur Complement in the inequality (16) obtaining the equivalent condition:

$$\Xi_1 + \Xi_2 \Xi_4^{-1} \Xi_2^T + \Xi_3^T \Xi_4 \Xi_3 < 0. \tag{18}$$

The above inequality can be rewritten as:

$$\Xi_1 + \tau \Omega < 0 \tag{19}$$

where

$$\Omega = \tilde{\Xi}_2 \Xi_4^{-1} \tilde{\Xi}_2^T + \tilde{\Xi}_3^T \Xi_4 \tilde{\Xi}_3, \tag{20}$$

$$\tilde{\Xi}_2 = \begin{bmatrix} \tilde{G}_1 & 0_{2\times 1} & 0_2 \\ 0_{2\times 1} & 0_{2\times 1} & 0_2 \\ 0_{2\times 1} & \tilde{G}_2 & \tilde{G}_3 \end{bmatrix}, \tilde{\Xi}_3 = \begin{bmatrix} 0_{1\times 2} & \tilde{H}_1 & 0_{1\times 2} \\ \tilde{H}_2 & 0_{1\times 2} & 0_{1\times 2} \\ 0_2 & \tilde{H}_3 & 0_2 \end{bmatrix},$$

$$\tilde{G}_1 = \frac{1}{4} \mu \delta_1 \begin{bmatrix} 0 \\ 1 \end{bmatrix}, \tilde{G}_2 = \delta_2 \lambda \sqrt{\tau} \begin{bmatrix} 1 \\ 0 \end{bmatrix}, \tilde{G}_3 = -\frac{1}{2} K_1 \delta_3 \lambda \sqrt{\tau} \cdot I_2,$$

$$\tilde{H}_1 = \begin{bmatrix} 1 & 0 \end{bmatrix}, \tilde{H}_2 = \sqrt{\tau} \begin{bmatrix} 1 & 0 \end{bmatrix}, \tilde{H}_3 = \sqrt{\tau} \begin{bmatrix} 1 & 0 \\ 0 & 2\frac{K_2}{K_1} \end{bmatrix}$$

[‡]The symbol (*) denotes the corresponding term induced by symmetry.

If τ is sufficiently small and $\Xi_1 < 0$, then the inequality (19) holds, as long as the term $\tau\Omega$ vanishes. On the other hand, from the definition of Ξ_1 in (17), note that the third row and column can be removed from the inequality $\Xi_1 < 0$ due to the fact that $\lambda > 0$, leading to:

$$\begin{bmatrix} -\lambda I_2 & \tilde{\Gamma}_1 + \lambda I_2 \\ (*) & -\lambda I_2 \end{bmatrix} < 0 \tag{21}$$

Applying Schur Complement, (21) is equivalent to:

$$-\lambda I_2 + \left(\tilde{\Gamma}_1 + \lambda I_2\right)\left(\lambda I_2\right)^{-1}\left(\tilde{\Gamma}_1 + \lambda I_2\right)^T < 0 \tag{22}$$

Expanding terms we have:

$$-\lambda I_2 + \tilde{\Gamma}_1\left(\lambda I_2\right)^{-1}\tilde{\Gamma}_1^T + \tilde{\Gamma}_1 + \tilde{\Gamma}_1^T + \lambda I_2 < 0 \tag{23}$$

which can be simplified as:

$$\lambda^{-1}\tilde{\Gamma}_1\tilde{\Gamma}_1^T + \tilde{\Gamma}_1 + \tilde{\Gamma}_1^T < 0 \tag{24}$$

Choosing a sufficiently large value for λ and taking into account the definition of $\tilde{\Gamma}_1$ in (17), we have that (24) holds if:

$$diag\left(-\frac{1}{2}K_1, \quad -\mu K_2\right) < 0 \tag{25}$$

Finally, note that (25) always holds for any positive K_1, K_2 since $\mu > 0$. Therefore, the fulfilment of (25) implies (16) when τ is small enough. $\square$

Given a multiagent system, note that Theorem 1 requires a prior knowledge of τ to check its stability. From the basis that there exists a small enough value for τ such that the LMI (16) holds (Corollary 1), we propose the following algorithm to easily obtain the worst-case point-to-point delay τ with a pre-specified tolerance error ϵ_τ:

Algorithm 1

- (i) Set $k = 0$ and some $\Delta_\tau > 0$. Choose $\tau^{(0)}$ sufficiently small such that the LMI (16) is verified.
- (ii) Set $\tau^{(k+1)} = \tau^{(k)} + \Delta_\tau$, $k := k + 1$, and solve LMI's (16).
- (iii) If a feasible solution exists, go to step (ii). Otherwise, set $\Delta_\tau = \frac{1}{2}\Delta_\tau$ and go to step (iv).
- (iv) If $\Delta_\tau \leq \epsilon_\tau$ stop. Otherwise go to step (ii).

Remark 4

It is worth pointing out that one of the key advantages is that our algorithm can effectively be applied to large-scale systems, that is, the complexity of the proposed algorithm (number of involved decision variables and size of LMI (16)) is independent on the number of agents N. However, the price to pay is the conservatism on the estimation of τ. In other words, the obtained estimation for τ is expected to be conservative with respect to the actual worst-case point-to-point delay when N increases, as shown later through simulation results.

5. SIMULATION RESULTS

In this section, simulation results are given to show how the performance of the multiagent formation control system is affected by communication delays. For simplicity, the upper bound for each d_{ji} is chosen to be equal to the worst-case point-to-point delay: $d_{ji} = \tau$, $\forall j, i$. The maximum angular velocities are assumed to be bounded by $\sigma = 2\pi \, rad/s$. For the time simulations, the initial positions for all the agents are randomly established. The total relative formation index error e_c (%) is defined as $e_c(t) = 100\left(\frac{V(t)}{V(0)}\right)$, where $V(t)$ is the Lyapunov-Krasovskii functional candidate defined in (42). On the sequel, the parameter e_c will be used as a performance index of the speed of convergence.
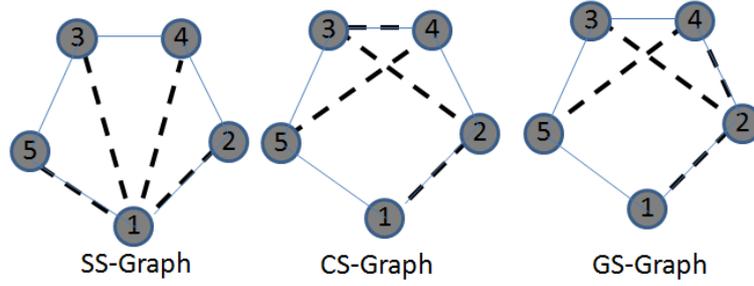
Figure 2. Prescribed target formation (continous-line) and the three communication graphs (dashed-line), considered in Simulation 1. (from left to right: *star-shaped* (SS) graph, *chain-shaped* (CS) graph and *generic-shaped* (GS) graph).

5.1. Simulation 1

Consider a multiagent system formed by $N = 5$ unicycle agents and the control gains $K_1 = 0.1$, $K_2 = 0.25$. Algorithm 1 gives a worst-case point-to-point delay $\tau = 26ms$ finding a feasible solution for the inequality (16) with $\lambda = 0.0300$, $\mu = 0.0781$, $\varepsilon_1 = 32.5453$, and $\varepsilon_2 = 0.4749$.

Simulation results: In this case, a pentagonal formation of radius 6m and the following three communication graphs (see Fig. 2) are considered. The corresponding adjacency matrix, defined in (5), and the matrix $\tilde{A}$ defined in (8), are respectively depicted below (from left to right: *star-shaped* (SS) graph, *chain-shaped* (CS) graph and *generic-shaped* (GS) graph:

$$\mathcal{A}^{(SS)} = \begin{bmatrix} 0 & 1 & 1 & 1 & 1 \\ 1 & 0 & 0 & 0 & 0 \\ 1 & 0 & 0 & 0 & 0 \\ 1 & 0 & 0 & 0 & 0 \\ 1 & 0 & 0 & 0 & 0 \end{bmatrix}, \mathcal{A}^{(CS)} = \begin{bmatrix} 0 & 1 & 0 & 0 & 0 \\ 1 & 0 & 1 & 0 & 0 \\ 0 & 1 & 0 & 1 & 0 \\ 0 & 0 & 1 & 0 & 1 \\ 0 & 0 & 0 & 1 & 0 \end{bmatrix}, \mathcal{A}^{(GS)} = \begin{bmatrix} 0 & 1 & 0 & 0 & 0 \\ 1 & 0 & 1 & 1 & 0 \\ 0 & 1 & 0 & 0 & 0 \\ 0 & 1 & 0 & 0 & 1 \\ 0 & 0 & 0 & 1 & 0 \end{bmatrix}$$

$$\tilde{\mathcal{A}}^{(SS)} = \begin{bmatrix} 0 & 1 & 0 & 0 & 0 \\ 1 & 0 & 0 & 0 & 0 \\ 1 & 0 & 0 & 0 & 0 \\ 1 & 0 & 0 & 0 & 0 \\ 1 & 0 & 0 & 0 & 0 \end{bmatrix}, \tilde{\mathcal{A}}^{(CS)} = \begin{bmatrix} 0 & 1 & 0 & 0 & 0 \\ 1 & 0 & 0 & 0 & 0 \\ 0 & 1 & 0 & 0 & 0 \\ 0 & 0 & 1 & 0 & 0 \\ 0 & 0 & 0 & 1 & 0 \end{bmatrix}, \tilde{\mathcal{A}}^{(GS)} = \begin{bmatrix} 0 & 1 & 0 & 0 & 0 \\ 1 & 0 & 0 & 0 & 0 \\ 0 & 1 & 0 & 0 & 0 \\ 0 & 1 & 0 & 0 & 0 \\ 0 & 0 & 0 & 1 & 0 \end{bmatrix}$$

The trajectories followed by each agent, linear velocities, angular velocities, and total formation index error are depicted in Fig. 3-6 respectively for $\tau = 0s, 1.25s$ and $2.5s$. A time window of $100s$ have been established. In all the cases, it can be appreciated how the multiagent formation control system converges to the prescribed frame, even for delays much larger than the upper value for the worst-case point-to-point delay $\tau = 26ms$ obtained by Algorithm 1. This fact confirms the conservativeness of the estimation, as discussed in Remark 4. In particular, it can be seen that the angular velocity does not converge to zero when $\tau = 2.5s$ and the communication graph is star-shaped (see Fig. 5, upper-right corner). It means that, although the correct formation is achieved, the agents keep rotating in place (the problem of tracking the orientation ϕ_i has been left out of the scope of this paper, being matter of future research). It is also noteworthy that, although the formation is still achieved in this case, the multiagent system is near from the limit to be unstable (indeed, slightly greater values than $2.5s$ for τ leads the system to instability). In general, the overall system performance is degraded when the delay grows. It is reflected on the presence of abrupt modifications on the trajectories, forcing the presence of peaks on the angular velocity. This behaviour is more evident when the system is close to the limit of instability (see Fig. 5, upper-right corner).

5.2. Simulation 2

Consider a multiagent system formed by $N = 12$ unicycle agents and the control gains $K_1 = 1.5$, $K_2 = 2$. Algorithm 1 gives a worst-case point-to-point delay $\tau = 10ms$. A feasible solution for the inequality (16) exists with $\lambda = 0.3881$, $\mu = 0.2713$, $\varepsilon_1 = 3679.6$, and $\varepsilon_2 = 369.2501$.
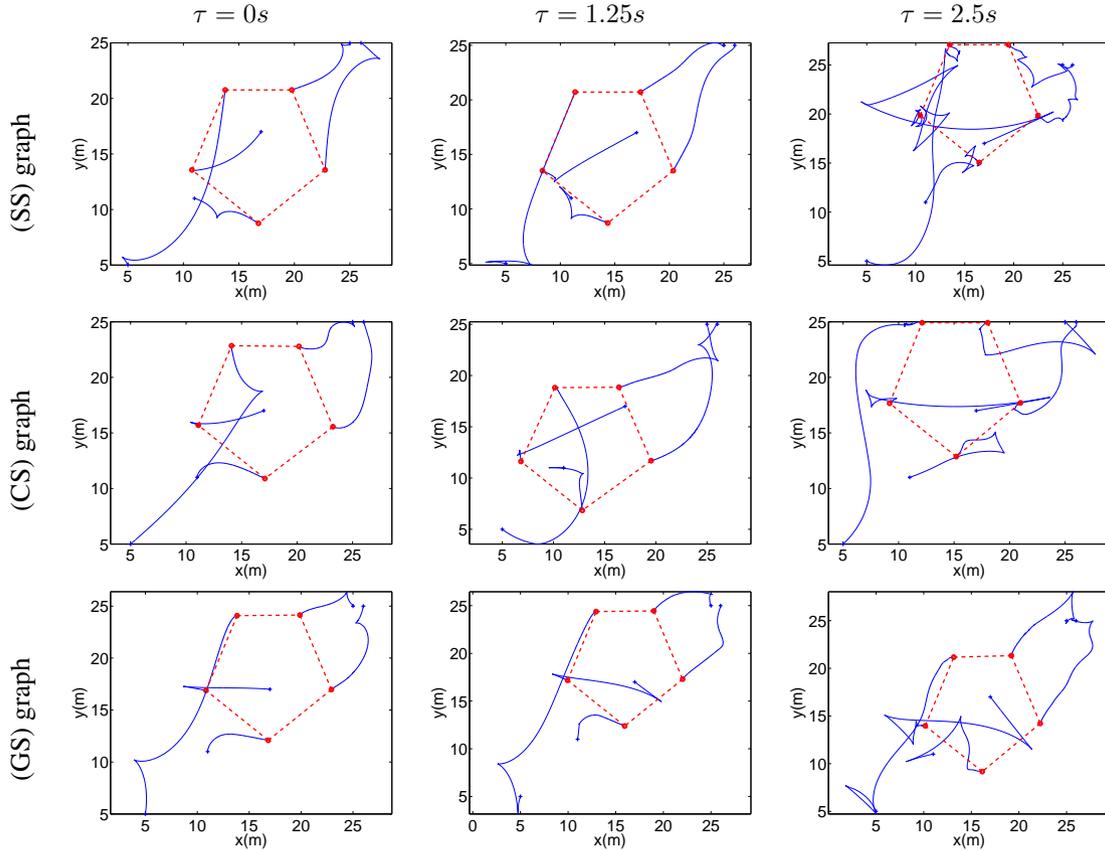
Figure 3. Simulation 1: Trajectories followed by each agent for different delays : Left column, $\tau = 0s$, Middle column, $\tau = 1.25s$, Right column, $\tau = 2.5s$. Upper row, *star-shaped* (SS) graph, Middle row, *chain-shaped* (CS) graph and Lower row *generic-shaped* (GS) graph.

Simulation results: In this case, we define a 4×3 rectangular grid formation with inter-agent distance of 6m. The communication graph (dotted-line) and the prescribed target formation to be reached (continous-line) are depicted in Fig. 7. The trajectories followed by each agent and the total formation index error are depicted in Fig. 8 (upper and lower row, respectively), with $\tau = 0ms$, $\tau = 85ms$ and $\tau = 170ms$ respectively. The delay of $170ms$ has been intentionally chosen to be on the limit of stability. In this case, simulation results reveal a drastic deterioration on the agent's trajectories, despite the target formation is achieved (see Fig.8, upper-right corner). Once again, the conservativeness of the estimation is shown by comparing the theoretical value $\tau = 10ms$ obtained from Algorithm 1 and the actual limit of $170ms$, obtained by simulation.

5.3. Simulation 3

In this example, we compare the worst-case point-to-point delay τ computed by algorithm 1 with the actual τ obtained by performing several simulations for different number of agents N (see Fig. 9). The worst-case point-to-point delay τ computed by algorithm 1 is the theoretical bound under which the system is guaranteed to be stable for any graph, target formation and initial condition. The actual τ (depicted with the symbol "*" in Fig. 9) is the maximum delay for stability obtained by performing a large number of simulations. For each simulation, the initial positions, the target formation and the connected graph are randomly generated. Then, we repeat each simulation by increasing τ from 0s until the limit value, in which the formation index error e_c is greater than 1%, after a sufficiently large time window of 400s. In all cases, the control gains are set to $K_1 = 3$ and $K_2 = 5.5$. It can be appreciated how both the theoretical bound for τ and the actual one diminish when the number
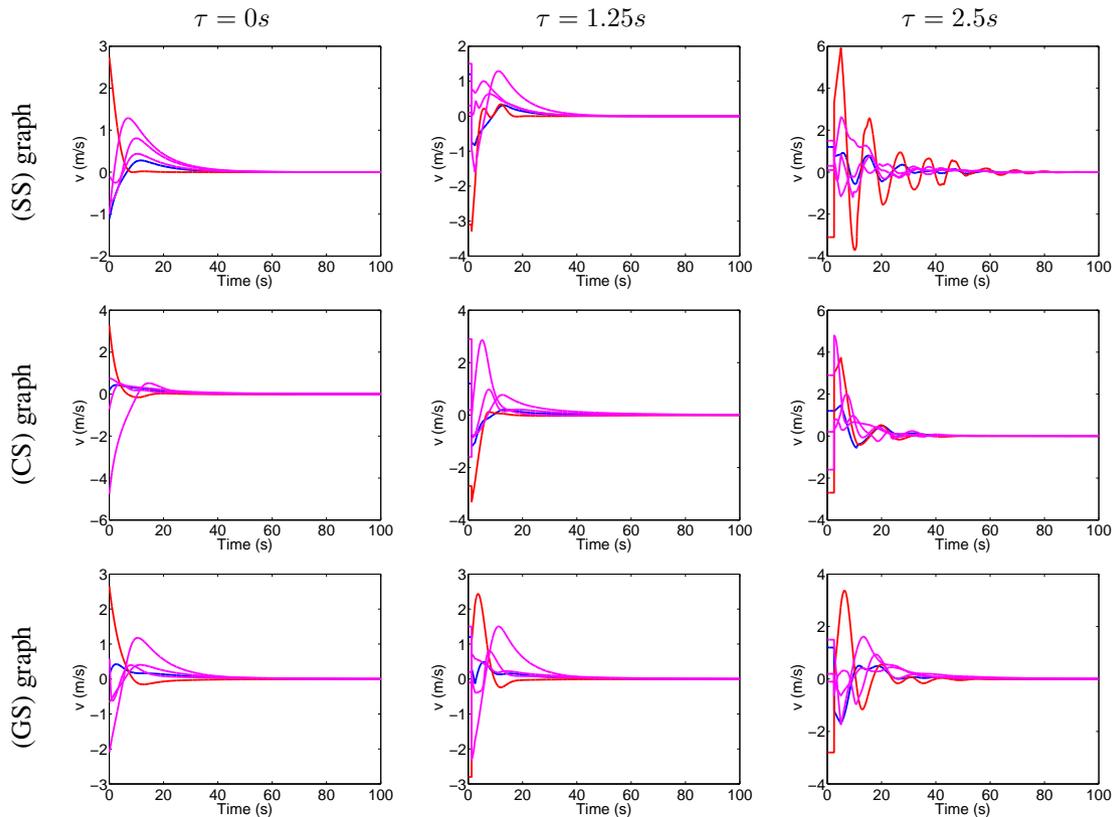
Figure 4. Simulation 1: Linear velocities v_i of each agent for different delays : Left column, $\tau = 0s$, Middle column, $\tau = 1.25s$, Right column, $\tau = 2.5s$. Upper row, *star-shaped* (SS) graph, Middle row, *chain-shaped* (CS) graph and Lower row *generic-shaped* (GS) graph.

of agents N increments. Note that, in all cases, the actual limit for τ is always greater than the theoretical bound for τ. This fact confirms the effectiveness of the proposed method. One possible future line of research is to investigate how to reduce the gap between the theoretical and actual bounds for τ, by including additional information (for instance, related with the communication graph through the adjacency matrix $\mathcal{A}$, or the prescribed target formation) by keeping a reasonable trade-off between accuracy and complexity on the algorithms.

6. DISCUSSION AND CONCLUSION

We have presented a sufficient condition based on LMI to ensure the asymptotic convergence of coordinate-free nonholonomic multiagent formation control systems subject to communication delays, given an upper bound for the worst-case point-to-point delay. Moreover, we have developed an algorithm to obtain the worst-case point-to-point delay. Although the estimation may be quite conservative in some cases, it is noteworthy that the complexity of the given method (size and number of decision variables on the LMI's to be solved) does not depend on the number of agents N. Therefore, it can effectively be applied to large-scale systems. In addition, the communication graph is only required to be connected. One appealing extension of this work is to extend the analysis to time-varying delays or switching topologies.
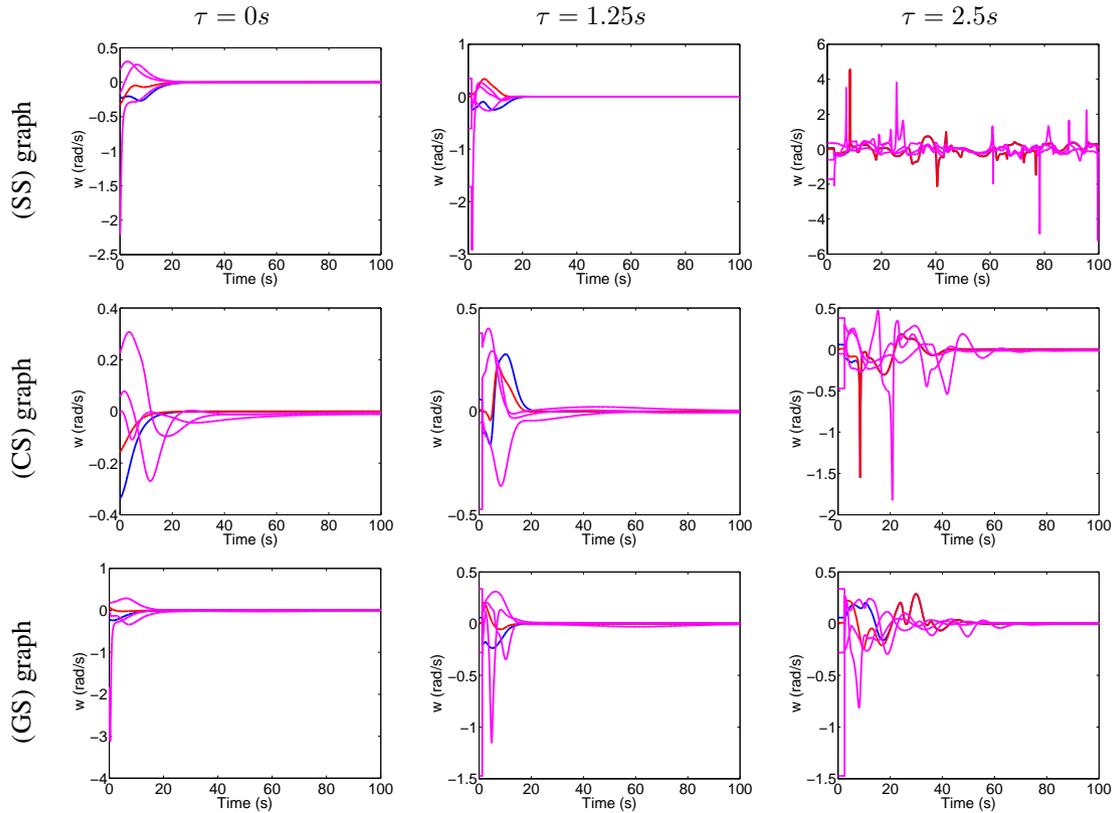
Figure 5. Simulation 1: Angular velocities w_i of each agent for different delays : Left column, $\tau = 0s$, Middle column, $\tau = 1.25s$, Right column, $\tau = 2.5s$. Upper row, *star-shaped* (SS) graph, Middle row, *chain-shaped* (CS) graph and Lower row *generic-shaped* (GS) graph.

ACKNOWLEDGEMENT

REFERENCES

1. Oh KK, Park MC, Ahn HS. A survey of multi-agent formation control. *Automatica* 2015; **53**:424–440.
2. Ren W, Atkins E. Distributed multi-vehicle coordinated control via local information exchange. *International Journal of Robust and Nonlinear Control* 2007; **17**(10-11):1002–1033.
3. Ren W. Consensus strategies for cooperative control of vehicle formations. *IET Control Theory & Applications* 2007; **1**(2):505–512.
4. Abdessameud A, Tayebi A. Formation control of vtol unmanned aerial vehicles with communication delays. *Automatica* 2011; **47**(11):2383–2394.
5. Dong X, Yu B, Shi Z, Zhong Y. Time-varying formation control for unmanned aerial vehicles: Theories and applications. *IEEE Transactions on Control Systems Technology* 2015; **23**(1):340–348.
6. Zavlanos MM, Pappas GJ. Distributed formation control with permutation symmetries. *46th IEEE Conference on Decision and Control*, New Orleans, LA, Dec 2007; 2894–2899.
7. Sabattini L, Secchi C, Fantuzzi C. Arbitrarily shaped formations of mobile robots: artificial potential fields and coordinate transformation. *Autonomous Robots* 2011; **30**(4):385–397.
8. Oh KK, Ahn HS. Formation control of mobile agents based on inter-agent distance dynamics. *Automatica* 2011; **47**(10):2306–2312.
9. Dimarogonas DV, Kyriakopoulos KJ. A connection between formation infeasibility and velocity alignment in kinematic multi-agent systems. *Automatica* 2008; **44**(10):2648–2654.
10. Coogan S, Arcak M. Scaling the size of a formation using relative position feedback. *Automatica* 2012; **48**(10):2677–2685.
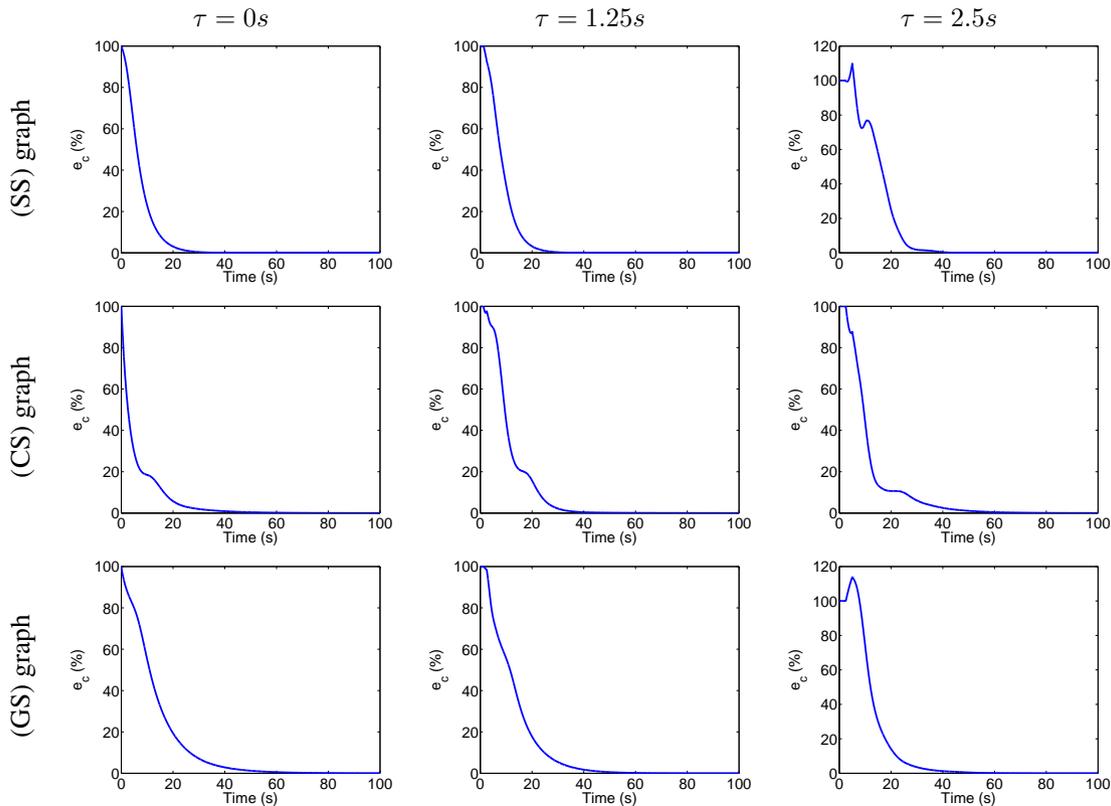
Figure 6. Simulation 1: Relative position error $e_c = 100 \left(\frac{V(t)}{V(0)} \right)$ (%), after 100s of time simulation: Left column, $\tau = 0s$, Middle column, $\tau = 1.25s$, Right column, $\tau = 2.5s$. Upper row, *star-shaped* (SS) graph, Middle row, *chain-shaped* (CS) graph and Lower row *generic-shaped* (GS) graph.
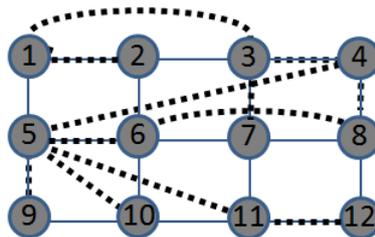

Figure 7. Prescribed target formation (continous-line) and the communication graph (dashed-line) considered in Simulation 2.

11. Oh KK, Ahn HS. Formation control and network localization via orientation alignment. *IEEE Transactions on Automatic Control* 2014; **59**(2):540–545.
12. Gu K, Chen J, Kharitonov VL. *Stability of time-delay systems*. Springer Science & Business Media, 2003.
13. Richard JP. Time-delay systems: an overview of some recent advances and open problems. *Automatica* 2003; **39**(10):1667–1694.
14. Chung SJ, Ahsun U, Slotine JJE. Application of synchronization to formation flying spacecraft: Lagrangian approach. *Journal of Guidance, Control, and Dynamics* 2009; **32**(2):512.
15. Liu Z, Chen W, Lu J, Wang H, Wang J. Formation control of mobile robots using distributed controller with sampled-data and communication delays. *IEEE Transactions on Control Systems Technology* 2016; **24**(6):2125–2132.
16. Aranda M, López-Nicolás G, Sagüés C, Zavlanos MM. Coordinate-free formation stabilization based on relative position measurements. *Automatica* 2015; **57**:11–20.
17. Dong X, Han L, Li Q, Ren Z. Time-varying formation control for double-integrator multi-agent systems with jointly connected topologies. *International Journal of Systems Science* 2016; **47**(16):3829–3838.
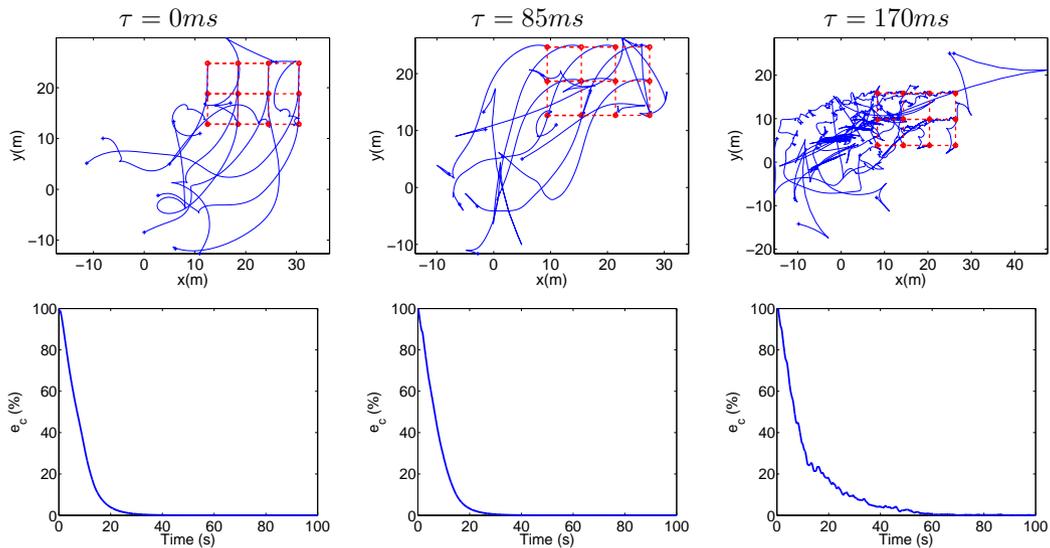
Figure 8. Simulation 2: Upper row: Trajectories followed by each agent, Lower row 4: Error $e_c(\%)$. Time window for simulation: 100s. Left column, $\tau = 0ms$, Middle column, $\tau = 85ms$, Right column, $\tau = 170ms$
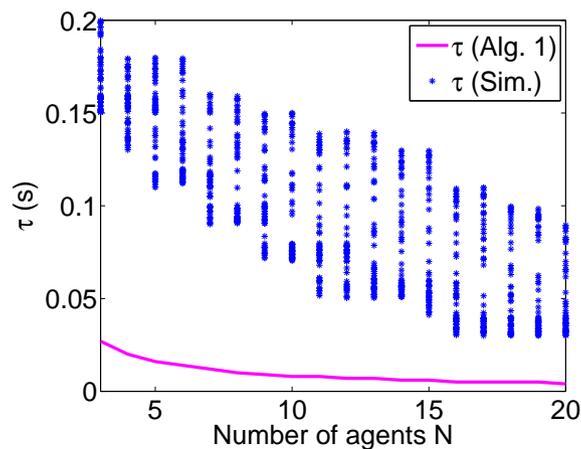

Figure 9. Comparison of the worst-case point-to-point delay τ obtained by algorithm 1 (continuous line) vs the actual τ (dotted line), obtained by performing a large number of simulations with different target formations and graphs. The control gains in all cases are $K_1 = 3$ and $K_2 = 5.5$.

18. Dong X, Li Q, Ren Z, Zhong Y. Formation-containment control for high-order linear time-invariant multi-agent systems with time delays. *Journal of the Franklin Institute* 2015; **352**(9):3564–3584.
19. Shang Y, Hou D, Gao F. Global output feedback stabilization of nonholonomic chained form systems with communication delay. *IAENG International Journal of Applied Mathematics* 2016; **46**(3):367–371.
20. Liu ZG, Wu YQ, Sun ZY. Output feedback control for a class of high-order nonholonomic systems with complicated nonlinearity and time-varying delay. *Journal of the Franklin Institute* 2017; **354**(11):4289–4310.
21. Cepeda-Gomez R, Perico LF. Formation control of nonholonomic vehicles under time delayed communications. *IEEE Transactions on Automation Science and Engineering* 2015; **12**(3):819–826.
22. Aranda M, López-Nicolás G, Sagüés C, Zavlanos MM. Distributed formation stabilization using relative position measurements in local coordinates. *IEEE Transactions on Automatic Control* 2016; **61**(12):3925–3935.
23. Kharitonov V, Zhabko A. Lyapunov–krasovskii approach to the robust stability analysis of time-delay systems. *Automatica* 2003; **39**(1):15–20.
24. Boyd S, El Ghaoui L, Feron E, Balakrishnan V. Linear matrix inequalities in system and control theory. *Philadelphia, PA: SIAM* 1994; .
25. Nesterov Y, Nemirovskii A. *Interior-point polynomial algorithms in convex programming*. Philadelphia, PA: SIAM, 1994, 1994.
26. Gahinet P, Nemirovski A, Laub A, Chilali M. *LMI* control toolbox. *The MathWorks, Inc.* 1995; .

27. Labit Y, Peaucelle D, Henrion D. Sedumi interface 1.02: a tool for solving LMI problems with sedumi. *IEEE International Symposium on Computer Aided Control System Design*, Glasgow, Scotland, Sept 2002; 272–277.
28. Brockett R. Asymptotic stability and feedback stabilization. *Differential geometric control theory* 1983; **27**(1):181–191.
29. Astolfi A. Exponential stabilization of a wheeled mobile robot via discontinuous control. *ASME Journal on Dynamic Systems, Measurement, and Control,* 1999; **121**(1):121–126.
30. Pathak K, Agrawal SK. An integrated path-planning and control approach for nonholonomic unicycles using switched local potentials. *IEEE Transactions on Robotics* 2005; **21**(6):1201–1208.
31. Ailon A, Zohar I. Control strategies for driving a group of nonholonomic kinematic mobile robots in formation along a time-parameterized path. *IEEE/ASME Transactions on Mechatronics* 2012; **17**(2):326–336.
32. Tayefi M, Geng Z, Peng X. Coordinated tracking for multiple nonholonomic vehicles on se (2). *Nonlinear Dynamics* 2017; **87**(1):665–675.
33. Dimarogonas DV, Kyriakopoulos KJ. On the rendezvous problem for multiple nonholonomic agents. *IEEE Transactions on automatic control* 2007; **52**(5):916–922.
34. Jafarian M. Robust consensus of unicycles using ternary and hybrid controllers. *International Journal of Robust and Nonlinear Control* 2017; **27**(17):4013–4034.
35. Cheng L, Hou ZG, Tan M, Lin Y, Zhang W. Neural-network-based adaptive leader-following control for multiagent systems with uncertainties. *IEEE Transactions on Neural Networks* 2010; **21**(8):1351–1358.
36. Mei J, Ren W, Li B, Ma G. Distributed containment control for multiple unknown second-order nonlinear systems with application to networked lagrangian systems. *IEEE transactions on neural networks and learning systems* 2015; **26**(9):1885–1899.

7. APPENDIX

7.1. *Proof of Lemma 2*

From the definition of ρ_{ji} in (3), we have that:

$$\dot{\rho}_{ji} = \frac{(q_{j,x} - q_{i,x} - c_{ji,x})(\dot{q}_{j,x} - \dot{q}_{i,x}) + (q_{j,y} - q_{i,y} - c_{ji,y})(\dot{q}_{j,y} - \dot{q}_{i,y})}{\sqrt{((q_{j,x} - q_{i,x}) - c_{ji,x})^2 + ((q_{j,y} - q_{i,y}) - c_{ji,y})^2}}. \tag{26}$$

From (1) and the definition of the angle ψ_{ji} below (4) we have:

$$\dot{\rho}_{ji} = cos(\psi_{ji})\left(v_j cos(\phi_j) - v_i cos(\phi_i)\right) + sin(\psi_{ji})\left(v_j sin(\phi_j) - v_i sin(\phi_i)\right). \tag{27}$$

Rearranging terms in v_j and v_i, the above expression yields:

$$\dot{\rho}_{ji} = \left(cos(\psi_{ji})cos(\phi_j) + sin(\psi_{ji})sin(\phi_j)\right)v_j \\ - \left(cos(\psi_{ji})cos(\phi_i) + sin(\psi_{ji})sin(\phi_i)\right)v_i. \tag{28}$$

From $cos(a + b) = cos(a)cos(b) - sin(a)sin(b)$, the expression (28) can be simplified as:

$$\dot{\rho}_{ji} = cos(\alpha_{jji})v_j - cos(\alpha_{iji})v_i. \tag{29}$$

Taking into account that $\psi_{ji} = \psi_{ij} + \pi$ we have that $cos(\alpha_{jji}) = -cos(\alpha_{jij})$. Then, the above expression is equivalent to (14). The proof is completed.

7.2. *Proof of Lemma 3*

Note from the definition of α_{kji} in (4) that:

$$\dot{\alpha}_{kji} = \dot{\phi}_k - \dot{\psi}_{ji} = \omega_k - \dot{\psi}_{ji}. \tag{30}$$

The time derivative of ψ_{ji} is:

$$\dot{\psi}_{ji} = \frac{(\dot{q}_{j,y} - \dot{q}_{i,y})(q_{j,x} - q_{i,x} - c_{ji,x}) - (q_{j,y} - q_{i,y} - c_{ji,y})(\dot{q}_{j,x} - \dot{q}_{i,x})}{(q_{j,x} - q_{i,x} - c_{ji,x})^2 + (q_{j,y} - q_{i,y} - c_{ji,y})^2}. \tag{31}$$

The above expression can be rewritten as:

$$\dot{\psi}_{ji} = \frac{1}{\rho_{ji}}\left(cos(\psi_{ji})\left(v_j sin(\phi_j) - v_i sin(\phi_i)\right) - sin(\psi_{ji})\left(v_j cos(\phi_j) - v_i cos(\phi_i)\right)\right). \tag{32}$$

Rearranging terms in v_j and v_i, the above expression yields:

$$\dot{\psi}_{ji} = \frac{1}{\rho_{ji}} \left(cos(\psi_{ji})sin(\phi_j) - sin(\psi_{ji})cos(\phi_j)\right) v_j \tag{33}$$
$$- \left(cos(\psi_{ji})sin(\phi_i) - sin(\psi_{ji})cos(\phi_i)\right) v_i.$$

Applying the identity: $sin(a-b) = sin(a)cos(b) - sin(b)cos(a)$, the above expression can be written in compact form as:

$$\dot{\psi}_{ji} = \frac{1}{\rho_{ji}} sin(\alpha_{jji})v_j - \frac{1}{\rho_{ji}} sin(\alpha_{iji})v_i. \tag{34}$$

From the fact that $\alpha_{iji} = \alpha_{jij} + \pi$ we have that $sin(\alpha_{jji}) = -sin(\alpha_{jij})$. Therefore (34) is equivalent to:

$$\dot{\psi}_{ji} = -\frac{1}{\rho_{ji}} sin(\alpha_{jij})v_j - \frac{1}{\rho_{ji}} sin(\alpha_{iji})v_i. \tag{35}$$

Finally, replacing $\dot{\psi}_{ji}$ into (30) we obtain (15). The proof is completed.

7.3. Proof of Theorem 1

First, let us define the augmented vectors containing all the relative distance errors and the angular misalignment errors (ρ_{ji} and α_{iji} respectively), where $[i,j] \in [1,...,N] \times [1,...,N]$, $i \neq j$:

$$\bar{\rho} = \begin{bmatrix} \rho_{21} & \rho_{31} & \cdots & \rho_{N1} & \rho_{12} & \rho_{32} & \cdots & \rho_{N,N-1} \end{bmatrix}^T, \tag{36}$$
$$\bar{\alpha} = \begin{bmatrix} \alpha_{121} & \alpha_{131} & \cdots & \alpha_{1N1} & \alpha_{212} & \alpha_{232} & \cdots & \alpha_{N-1,N,N-1} \end{bmatrix}^T.$$

Applying lemmas 2 and 3, an augmented state-space model for the kinematics of the overall formation control system (1) can be written as:

$$\frac{d}{dt}\begin{bmatrix} \bar{\rho} \\ \bar{\alpha} \end{bmatrix} = \begin{bmatrix} -\mathcal{C} & 0 \\ \mathcal{RS} & \bar{\mathcal{L}}^T \end{bmatrix} \begin{bmatrix} \bar{v} \\ \bar{w} \end{bmatrix}, \tag{37}$$

where $\bar{\rho}$ and $\bar{\alpha}$ are defined in (36), and

$$\mathcal{C} = \bar{\mathcal{F}} \cdot diag\left(f_c(\bar{\alpha})\right) \bar{\mathcal{L}}^T, \quad \bar{\mathcal{R}} = diag\left(f_i\left(\bar{\rho}\right)\right) \tag{38}$$
$$\mathcal{S} = \bar{\mathcal{F}} \cdot diag\left(f_s(\bar{\alpha})\right) \bar{\mathcal{L}}^T, \quad \bar{\mathcal{L}} = \underbrace{I_N \otimes \mathbf{1_{1 \times N-1}}}_{\{0,1\}^{N \times N(N-1)}},$$

$$\bar{\mathcal{F}} = \bar{\mathcal{F}}^T = [F_{ij}]_{N,N}, \qquad F_{ij} = \begin{cases} I_{N-1} & if\ i=j \\ \left[f_{mn}^{(i,j)}\right]_{N-1,N-1} & if\ j>i \\ F_{ji}^T & if\ j<i \end{cases}$$

$$f_{mn}^{(i,j)} = \begin{cases} f_{mn}^{(i,j)} = 1 & if\ m=j-1\ and\ n=i \\ f_{mn}^{(i,j)} = 0 & otherwise \end{cases},$$

$$\bar{v}^T = \begin{bmatrix} v_1 & v_2 & \cdots & v_N \end{bmatrix}, \quad \bar{w}^T = \begin{bmatrix} w_1 & w_2 & \cdots & w_N \end{bmatrix},$$

being $f_c(.)$, $f_s(.)$ and $f_i(.)$ the following operators $\mathcal{R}^{\bar{N}} \rightarrow \mathcal{R}^{\bar{N}}$:

$$f_c(\varsigma) = \begin{bmatrix} cos(\varsigma_1) & \cdots & cos(\varsigma_{\bar{N}}) \end{bmatrix}, \tag{39}$$
$$f_s(\varsigma) = \begin{bmatrix} sin(\varsigma_1) & \cdots & sin(\varsigma_{\bar{N}}) \end{bmatrix},$$
$$f_i(\varsigma) = \begin{bmatrix} \frac{1}{\varsigma_1} & \cdots & \frac{1}{\varsigma_{\bar{N}}} \end{bmatrix},$$

where $\bar{N} = N(N-1)$ and $\varsigma = [\varsigma_1, ..., \varsigma_{\bar{N}}]$ is any input argument. Also, let introduce the auxiliary terms:

$$\xi_1 = \mathcal{C}^T \bar{\mathcal{A}} \bar{\rho}, \qquad \xi_2 = f_s\left(\bar{\mathcal{L}} \bar{\tilde{\mathcal{A}}} \bar{\alpha}\right) \tag{40}$$

From the above notation, the control law (7) can be written in compact form as:

$$\bar{v} = \frac{1}{2} K_1 \underbrace{\left(\mathcal{C}^{dT} \bar{\mathcal{A}} \bar{\rho}^d\right)}_{\xi_1^d} \tag{41}$$

$$\bar{w} = -K_2 \underbrace{f_s\left(\bar{\mathcal{L}} \bar{\tilde{\mathcal{A}}} \bar{\alpha}^d\right)}_{\xi_2^d} - \bar{\mathcal{L}} \bar{\tilde{\mathcal{A}}} \bar{\mathcal{R}}^d \mathcal{S}^d \bar{v}^d,$$

where the superindex d denotes that all the involved time-dependent terms are affected by time-delays: $\bar{\rho}^d = \begin{bmatrix} \rho_{21}(t - d_{21}) & \cdots & \rho_{ij}(t - d_{ij}) & \cdots & \rho_{N-1,N}(t - d_{N-1,N}) \end{bmatrix}^T$, etc.

Therefore, it can be proved the asymptotic convergence of the multiagent system (1) under the control law (7) through the augmented system formed by (37) and (41). To this end, given some scalars $\lambda, \mu > 0$, consider the following nonquadratic Lyapunov-Krasovskii functional:

$$V = V_a + \mu V_b + \lambda \tau \int_{-\tau}^{0} \int_{t+s}^{t} \dot{\xi}^T(s) \dot{\xi}(s) ds dt, \tag{42}$$

$$\xi^T = \begin{bmatrix} \xi_1^T, & \xi_2^T \end{bmatrix},$$

where $\tau > 0$ is the worst-case point-to-point delay, ξ_1 and ξ_2 are defined in (40), and

$$V_a = \frac{1}{2} \sum_{i=1}^{N} \sum_{j=1}^{N} a_{ij} \rho_{ij}^2, \quad V_b = \sum_{i=1}^{N} \sum_{j=1}^{N} \tilde{a}_{ij} \left(1 - cos(\alpha_{iji})\right) \tag{43}$$

Note from (43) that $V_a > 0, \forall \rho_{ij} \neq 0 \ / \ a_{ij} = 1$, where a_{ij} are the coefficients of the adjacency matrix corresponding to the indices i and j. Also, note that $V_b \geq 0, \ \forall \alpha_{iji}$. Therefore, taking into account that $\lambda > 0$ and $\mu > 0$, it can be deduced that the functional V in (42) is positive definite.

Using the notation (38), and taking into account from (10) that $\sum_{i=1}^{N} \sum_{j=1}^{N} \tilde{a}_{ij} = N$, the functionals V_a and V_b can be written in compact form as:

$$V_a = \frac{1}{2} \bar{\rho}^T \bar{\mathcal{A}} \bar{\rho}, \quad V_b = N - \mathbf{1}_{1 \times N} \cdot f_c\left(\bar{\mathcal{L}} \bar{\tilde{\mathcal{A}}} \bar{\alpha}\right), \tag{44}$$

where

$$\bar{\mathcal{A}} = diag \begin{bmatrix} a_{21} & a_{31} & \cdots & a_{N1} & a_{12} & a_{32} & \cdots & a_{N,N-1} \end{bmatrix}, \tag{45}$$

$$\bar{\tilde{\mathcal{A}}} = diag \begin{bmatrix} \tilde{a}_{21} & \tilde{a}_{31} & \cdots & \tilde{a}_{N1} & \tilde{a}_{12} & \tilde{a}_{32} & \cdots & \tilde{a}_{N,N-1} \end{bmatrix}.$$

The inequality constraint obtained from the criterion $\dot{V} < 0$ is a sufficient condition for the asymptotic stability of the formation control system.

Note from (37) that:

$$\frac{d}{dt}\bar{\rho} = -\mathcal{C}\bar{v}, \qquad \frac{d}{dt}\bar{\alpha} = \bar{\mathcal{L}}^T \bar{w} + \bar{\mathcal{R}} \mathcal{S} \bar{v}. \tag{46}$$

From the above expressions, and taking into account that $\bar{\mathcal{L}} \bar{\tilde{\mathcal{A}}} \bar{\mathcal{L}}^T = I_N$, the time-derivative $\dot{V}$ renders:

$$\dot{V} = \dot{V}_a + \mu \dot{V}_b + \lambda \tau \frac{d}{dt} \left(\int_{-\tau}^{0} \int_{t+s}^{t} \dot{\xi}^T(s) \dot{\xi}(s) ds dt \right) \tag{47}$$

$$= -\bar{\rho}^T \bar{\mathcal{A}} \mathcal{C} \bar{v} + \mu \left(f_s \left(\bar{\mathcal{L}} \tilde{\bar{\mathcal{A}}} \bar{\alpha} \right) \right)^T \cdot \left(\bar{\mathcal{L}} \tilde{\bar{\mathcal{A}}} \left(\bar{\mathcal{L}}^T \bar{w} + \bar{\mathcal{R}} \mathcal{S} \bar{v} \right) \right)$$

$$+ \lambda \tau^2 \dot{\xi}^T \dot{\xi} - \lambda \tau \int_{t-\tau}^{t} \dot{\xi}^T(s) \dot{\xi}(s) ds$$

$$= -\bar{\rho}^T \bar{\mathcal{A}} \mathcal{C} \bar{v} + \mu \left(f_s \left(\bar{\mathcal{L}} \tilde{\bar{\mathcal{A}}} \bar{\alpha} \right) \right)^T \cdot \left(\bar{w} + \bar{\mathcal{L}} \tilde{\bar{\mathcal{A}}} \bar{\mathcal{R}} \mathcal{S} \bar{v} \right)$$

$$+ \lambda \tau^2 \dot{\xi}^T \dot{\xi} - \lambda \tau \int_{t-\tau}^{t} \dot{\xi}^T(s) \dot{\xi}(s) ds.$$

From $\bar{v}$ and $\bar{w}$ in (41), the definition of ξ_1, ξ_2 in (40), and $\dot{V}$ in (47), the condition $\dot{V} < 0$ leads to the following inequality:

$$-\frac{K_1}{2} \xi_1^T \xi_1^d - \mu K_2 \xi_2^T \xi_2^d \tag{48}$$

$$+ \mu \frac{K_1}{2} \xi_2^T \underbrace{\left(\bar{\mathcal{L}} \tilde{\bar{\mathcal{A}}} \bar{\mathcal{R}}^d \mathcal{S}^d - \bar{\mathcal{L}} \tilde{\bar{\mathcal{A}}} \bar{\mathcal{R}} \mathcal{S} \right)}_{\Psi_1} \xi_1^d$$

$$+ \lambda \tau^2 \dot{\xi}^T \dot{\xi} - \lambda \tau \int_{t-\tau}^{t} \dot{\xi}^T(s) \dot{\xi}(s) ds < 0.$$

The above expression can be written in compact form as:

$$\begin{bmatrix} \xi \\ \xi^d \end{bmatrix}^T \begin{bmatrix} 0_N & \Gamma_1 \\ \Gamma_1^T & 0_N \end{bmatrix} \begin{bmatrix} \xi \\ \xi^d \end{bmatrix} \tag{49}$$

$$+ \lambda \tau^2 \dot{\xi}^T \dot{\xi} - \lambda \tau \int_{t-\tau}^{t} \dot{\xi}^T(s) \dot{\xi}(s) ds < 0,$$

where

$$\Gamma_1 = \begin{bmatrix} -\frac{1}{4} K_1 \cdot I_N & 0_N \\ \frac{1}{4} \mu \Psi_1 & -\frac{1}{2} \mu K_2 \cdot I_N \end{bmatrix}, \ \Psi_1 = \bar{\mathcal{L}} \tilde{\bar{\mathcal{A}}} \bar{\mathcal{R}}^d \mathcal{S}^d - \bar{\mathcal{L}} \tilde{\bar{\mathcal{A}}} \bar{\mathcal{R}} \mathcal{S}. \tag{50}$$

To deal with the integral term in (49), by applying the Jensen Inequality we have that:

$$-\lambda \tau \int_{t-\tau}^{t} \dot{\xi}^T(s) \dot{\xi}(s) ds \leq -\lambda \left(\int_{t-\tau}^{t} \dot{\xi}(s) \right)^T \left(\int_{t-\tau}^{t} \dot{\xi}(s) \right) \tag{51}$$

$$= -\lambda(\xi - \xi^d)(\xi - \xi^d) = \begin{bmatrix} \xi \\ \xi^d \end{bmatrix}^T \begin{bmatrix} -\lambda I_N & \lambda I_N \\ \lambda I_N & -\lambda I_N \end{bmatrix} \begin{bmatrix} \xi \\ \xi^d \end{bmatrix}.$$

On the other hand, the time derivative $\dot{\xi}$ yields:

$$\dot{\xi} = \begin{bmatrix} \frac{d}{dt} \xi_1^T & \frac{d}{dt} \xi_2^T \end{bmatrix}^T, \tag{52}$$

where

$$\frac{d}{dt} \xi_1 = \frac{d}{dt} \left(\mathcal{C}^T \bar{\mathcal{A}} \bar{\rho} \right) = \frac{d}{dt} \left(\mathcal{C}^T \right) \bar{\mathcal{A}} \bar{\rho} + \mathcal{C}^T \bar{\mathcal{A}} \left(\frac{d}{dt} \bar{\rho} \right) \tag{53}$$

$$= \bar{\mathcal{L}} diag \left(f_s(\bar{\alpha}) \right) \cdot diag \left(\frac{d}{dt} \bar{\alpha} \right) \bar{\mathcal{F}}^T \bar{\mathcal{A}} \bar{\rho} + \mathcal{C}^T \bar{\mathcal{A}} \left(\frac{d}{dt} \bar{\rho} \right)$$

$$\frac{d}{dt} \xi_2 = diag \left(f_c \left(\bar{\mathcal{L}} \tilde{\bar{\mathcal{A}}} \bar{\alpha} \right) \right) \cdot \bar{\mathcal{L}} \tilde{\bar{\mathcal{A}}} \left(\frac{d}{dt} \bar{\alpha} \right).$$

Replacing $\bar{v}, \bar{w}$ defined in (41) into (46) we obtain:

$$\frac{d}{dt}\bar{\rho} = -\frac{K_1}{2}\mathcal{C}\xi_1^d, \qquad \frac{d}{dt}\bar{\alpha} = -K_2\bar{\mathcal{L}}^T\xi_2^d - \frac{K_1}{2}\left(\bar{\mathcal{L}}^T\bar{\mathcal{L}}\tilde{\bar{\mathcal{A}}}\bar{\mathcal{R}}^d\mathcal{S}^d - \bar{\mathcal{R}}\mathcal{S}\right)\xi_1^d. \tag{54}$$

Replacing $\frac{d}{dt}\bar{\rho}$ and $\frac{d}{dt}\bar{\alpha}$ from (54) into (53), and taking into account again that $\bar{\mathcal{L}}\tilde{\bar{\mathcal{A}}}\bar{\mathcal{L}}^T = I_N$, we obtain:

$$\frac{d}{dt}\xi_1 = \Psi_2\xi_1 - \frac{K_1}{2}\mathcal{C}^T\bar{\mathcal{A}}\mathcal{C}\xi_1^d \tag{55}$$

$$\frac{d}{dt}\xi_2 = -K_2 diag\left(f_c\left(\bar{\mathcal{L}}\tilde{\bar{\mathcal{A}}}\bar{\alpha}\right)\right)\xi_2^d$$

$$- \frac{K_1}{2}diag\left(f_c\left(\bar{\mathcal{L}}\tilde{\bar{\mathcal{A}}}\bar{\alpha}\right)\right)\underbrace{\left(\bar{\mathcal{L}}\tilde{\bar{\mathcal{A}}}\bar{\mathcal{R}}^d\mathcal{S}^d - \bar{\mathcal{L}}\tilde{\bar{\mathcal{A}}}\bar{\mathcal{R}}\mathcal{S}\right)}_{\Psi_1}\xi_1^d.$$

Therefore, the above expression can be written in matricial form as:

$$\dot{\xi} = \Gamma_2\xi + \Gamma_3\xi^d, \tag{56}$$

where

$$\Gamma_2 = \begin{bmatrix} \Psi_2 & 0_N \\ 0_N & 0_N \end{bmatrix}, \tag{57}$$

$$\Gamma_3 = \begin{bmatrix} -\frac{K_1}{2}\mathcal{C}^T\bar{\mathcal{A}}\mathcal{C} & 0_N \\ -\frac{K_1}{2}diag\left(f_c\left(\bar{\mathcal{L}}\tilde{\bar{\mathcal{A}}}\bar{\alpha}\right)\right)\Psi_1 & -K_2 diag\left(f_c\left(\bar{\mathcal{L}}\tilde{\bar{\mathcal{A}}}\bar{\alpha}\right)\right) \end{bmatrix},$$

and Ψ_2 is a time-varying matrix which satisfies:

$$\Psi_2\mathcal{C}^T = \bar{\mathcal{L}}diag\left(f_s(\bar{\alpha})\right)\cdot diag\left(\frac{d}{dt}\bar{\alpha}\right)\bar{\mathcal{F}}^T. \tag{58}$$

Replacing from (51) and (56) into (48) and rearranging terms, we obtain the following inequality:

$$\dot{V} \le \begin{bmatrix} \xi \\ \xi^d \end{bmatrix}^T \left(\begin{bmatrix} -\lambda I_{2N} & \Gamma_1 + \lambda I_{2N} \\ (*) & -\lambda I_{2N} \end{bmatrix} + \begin{bmatrix} \Gamma_2^T \\ \Gamma_3^T \end{bmatrix} \left(\lambda\tau^2\cdot I_N\right) \begin{bmatrix} \Gamma_2 & \Gamma_3 \end{bmatrix} \right) \begin{bmatrix} \xi \\ \xi^d \end{bmatrix} < 0, \tag{59}$$

which is fulfilled $\forall\xi, \xi_d \ne 0$ if

$$\begin{bmatrix} -\lambda I_{2N} & \Gamma_1 + \lambda I_{2N} \\ (*) & -\lambda I_{2N} \end{bmatrix} + \begin{bmatrix} \Gamma_2^T \\ \Gamma_3^T \end{bmatrix} \left(\lambda\tau^2\cdot I_N\right) \begin{bmatrix} \Gamma_2 & \Gamma_3 \end{bmatrix} < 0. \tag{60}$$

From the fact that $\lambda\tau^2 > 0$, we apply Schur Complement obtaining that (60) is equivalent to:

$$\begin{bmatrix} -\lambda I_{2N} & \Gamma_1 + \lambda I_{2N} & \lambda\tau^2\Gamma_2^T \\ (*) & -\lambda I_{2N} & \lambda\tau^2\Gamma_3^T \\ (*) & (*) & -\lambda\tau^2 I_{2N} \end{bmatrix} < 0. \tag{61}$$

Now, let us write the terms $\Gamma_1, \lambda\tau^2\Gamma_2$ and $\lambda\tau^2\Gamma_3$ on the following form:

$$\Gamma_1 = \left(\tilde{\Gamma}_1 \otimes I_N\right) + \left(G_1 \otimes I_N\right)\underbrace{\left(\frac{1}{\delta_1\tau}\Psi_1\right)}_{\Delta_1(t)}\left(H_1 \otimes I_N\right), \tag{62}$$

$$\lambda\tau^2\Gamma_2 = \left(G_2 \otimes I_N\right)\underbrace{\left(\frac{1}{\delta_2}\Psi_2\right)}_{\Delta_2(t)}\left(H_2 \otimes I_N\right),$$

$$\lambda\tau^2\Gamma_3 = \left(G_3 \otimes I_N\right)\underbrace{\left(\delta_3\Psi_3\right)}_{\Delta_3(t)}\left(H_3 \otimes I_N\right),$$

$$\Psi_3 = \begin{bmatrix} \mathcal{C}^T\bar{\mathcal{A}}\mathcal{C} & diag(f_c(\bar{\alpha}))\Psi_1 \\ 0_N & diag(f_c(\bar{\alpha})) \end{bmatrix},$$

where the matrices $\Delta_i(t), i = 1, 2, 3$ are time-varying matrices which satisfy $\Delta_i^T(t)\Delta_i(t) \leq I, \ \forall t$, taking into account, from the boundedness of the coefficients of matrices Ψ_1, Ψ_2, Ψ_3 in (50), (58) and (62), and Assumption 3, that $||(1/\tau)\tilde{\Psi}_1||_\infty \leq \delta_1, \ ||\Psi_2||_\infty \leq \delta_2, \ ||\Psi_3||_\infty \leq \delta_3$. From (62) we can rewrite (61) as:

$$\Xi_1^* + \Xi_2^* \bar{\Delta}(t)\Xi_3^* + \Xi_3^{*T}\bar{\Delta}^T(t)\Xi_2^{*T} < 0, \tag{63}$$
$$\Xi_i^* = \Xi_i \otimes I_N, \ i = 1, 2, 3 \,,$$

where $\bar{\Delta}(t) = diag\left(\Delta_1(t), \Delta_2(t), \Delta_3(t)\right)$. Note from the block-diagonal structure of Ξ_4 and $\bar{\Delta}(t)$ that both matrices commute. Therefore, applying the Petersen Inequality in (63), we have that there exists some matrix $\Xi_4^* = \Xi_4 \otimes I_N < 0$ (which satisfies $\Xi_4\bar{\Delta}(t) = \bar{\Delta}(t)\Xi_4, \ \forall t \geq 0$) such that:

$$\Xi_1^* + \Xi_2^* \bar{\Delta}(t)\Xi_3^* + \Xi_3^{*T}\bar{\Delta}^T(t)\Xi_2^{*T} \leq \Xi_1^* - \Xi_2^*\Xi_4^{-*1}\Xi_2^{*T} - \Xi_3^{*T}\Xi_4^*\Xi_3^* < 0. \tag{64}$$

Finally, taking into account that $-\Xi_4^* > 0$, we can apply Schur Complement obtaining the inequality:

$$\begin{bmatrix} \Xi_1 & \Xi_2 & \Xi_3^T\Xi_4 \\ (*) & \Xi_4 & 0 \\ (*) & (*) & \Xi_4 \end{bmatrix} \otimes I_N < 0. \tag{65}$$

Applying Lemma 1, we have by congruence that the above inequality is equivalent to:

$$\mathcal{P}^T \left(I_N \otimes \begin{bmatrix} \Xi_1 & \Xi_2 & \Xi_3^T\Xi_4 \\ (*) & \Xi_4 & 0 \\ (*) & (*) & \Xi_4 \end{bmatrix} \right) \mathcal{P} < 0, \tag{66}$$

where $\mathcal{P}$ is a permutation matrix. Finally, it can be easily checked that the above inequality holds if (16) holds.